Solar 2008 Conf., San Diego, CA, American Solar Energy Society

FROM GLOBAL HORIZONTAL TO GLOBAL TILTED IRRADIANCE: HOW ACCURATE ARE SOLAR ENERGY ENGINEERING PREDICTIONS IN PRACTICE?

Christian A. Gueymard
Solar Consulting Services
P.O. Box 392
Colebrook, NH 03576, USA
Chris@SolarConsultingServices.com

ABSTRACT

Global radiation measured on fixed-tilt, sun-facing planes (40° and vertical) and a 2-axis tracker at NREL's Solar Radiation Research Lab. in Golden, CO is compared to predictions from ten transposition models, in combination with either optimal or suboptimal input data of horizontal irradiance. Suboptimal inputs are typically used in everyday engineering calculations, for which the necessary data are usually unavailable for the site under scrutiny, and must be estimated in some way. The performance of the transposition models is first evaluated for ideal conditions when optimal data are used. The performance of three direct/diffuse separation models is also evaluated. Finally, the performance of the resulting combinations is analyzed in a variety of situations. It is concluded that, for sunny sites such as this one, the Gueymard and Perez models provide the best estimates of global tilted irradiance only when optimal input data are used. When only global irradiance is known, the accuracy of the predicted tilted irradiance degrades significantly, and is conditioned by the local performance of the direct/diffuse separation method and, for vertical tilts in particular, by the accuracy in the ground reflection calculations.

1. INTRODUCTION

Accurate solar radiation resource data are necessary at various steps of the design, simulation, and performance evaluation of any project involving solar energy. Most solar energy systems are installed on either fixed tilted planes or tracking receivers. Similarly, glazed envelopes are installed vertically on the facades of buildings or at a variety of tilt angles in atria. Prediction of the global irradiance incident on such tilted surfaces is key to the evaluation of the solar resource and of the performance of all these systems. Because of the usual lack of measured data at the project's site, the solar resource needs to be modeled in most cases. Various models can be used, depending on the time resolution (e.g., hourly or monthly mean) and on the type of available input data (e.g., meteorological information or global irradiance on the horizontal). A typology of such models has been proposed recently (1). Monthly and hourly datasets of global radiation on the horizontal can now be found from various sources, such as NASA's SSE (2), NREL's NSRDB (3) and SWERA (4), SoDa (5), etc.

A previous study (6) showed that the accuracy of the predicted global tilted irradiance was a function of the experimental error in the global horizontal irradiance and of other factors, including ground albedo and frequency distribution of the diffuse/global ratio. The goal of the present contribution is to generalize these results by considering more variables, and to obtain results that can be related to the everyday practice of solar energy engineering. In this study, the overall performance of the radiation transposition between the horizontal and tilted planes is assessed in various ways. The literature is rich in investigations of this kind, e.g. (7-9). These contributions, however, focus on the performance of models that evaluate the tilted diffuse irradiance under *ideal* conditions only, i.e., when both the direct and diffuse horizontal components are measured at first-class experimental sites. These studies therefore fail to address the additional uncertainties introduced by the models used to separate the direct and diffuse horizontal components of global irradiance, or (*a fortiori*) those used to evaluate the global irradiance from meteorological inputs (such as cloud cover, aerosol turbidity, and water vapor).
In this respect, the present contribution offers some important improvements over the methodology that has been used in the literature up to now. These improvements include the use of:

- One-minute radiation data for enhanced time resolution, of importance for fast-responding (e.g., PV) systems
- Measured (each minute) *vs* estimated (using a fixed value, e.g., 0.2) ground albedo, for snow-free *vs* snow-covered ground conditions
- Accurate 1-minute cloud cover information.

These improvements provide the necessary elements to evaluate the uncertainty in the resulting global tilted irradiance under various conditions, from ideal (when the input direct and diffuse irradiances, and the ground albedo, are known very accurately) to most usual (when only the global horizontal irradiance is available).

2. TRANSPOSITION AND SEPARATION MODELS

The global irradiance, E_s, on a tilted plane, whose tilt is s degrees from the horizontal, can be evaluated from the classic equation:

$$E_s = E_{bn} \cos\theta + E_d R_d + \rho E R_r \quad (1)$$

where E_{bn} is the direct normal irradiance (DNI), E_d is the diffuse horizontal irradiance, E is the global horizontal irradiance, θ is the angle of incidence of the sun rays on the tilted plane, R_d is the diffuse transposition factor, ρ is the foreground's albedo, and R_r is the transposition factor for ground reflection. The irradiance components that appear on the right-hand-side of Eq. (1) are inter-related by the closure equation

$$E = E_{bn} \cos Z + E_d \quad (2)$$

where Z is the sun's zenith angle at any instant.
The calculation of the tilted direct component, $E_{bn} \cos\theta$, is purely geometric, and therefore straightforward and identical in all cases considered in what follows.
The evaluation of the ground-reflected diffuse irradiance is dependent on the factor R_r. Most studies consider that the ground reflection process is ideally isotropic, in which specific case R_r can be simplified into

$$R_r = (1 - \cos s)/2. \quad (2)$$

The foreground albedo can be estimated *a priori* (as in the general case), experimentally measured on site (as in this study), or modeled (10). The uncertainties associated with the use of approximate values of ρ and the isotropic approximation for R_r are discussed in Section 4.2.
The main unknown in Eq. (1) is normally R_d. If the diffuse radiance were ideally constant over the whole sky hemisphere, R_d would be easily obtained from the simple isotropic approximation

$$R_d = (1 + \cos s)/2. \quad (3)$$

In practice, a plane of tilt s facing the sun receives more diffuse radiation than a plane of same tilt in the opposite direction. Elaborate transposition models have been developed to estimate this anisotropic effect and calculate a refined value of R_d.
The transposition models selected here are those that are commonly used in solar energy engineering practice, for applications such as PV design (11) or building energy simulation (12). Besides the conventional isotropic approximation, the anisotropic diffuse models proposed by ASHRAE (13), Gueymard (10), Hay (14), Klucher (15), Muneer (16), Perez (17), Reindl (18), Skartveit (19) have been considered here, in addition to the composite algorithm known as "HDKR" (20).

To use Eq. (1), the radiative input must be in the form of separate measurements of the three components E_{bn}, E_d and E, or of only two of them through the additional use of Eq. (2). In many cases, only one irradiance component (usually E) is measured. In the majority of cases, it is not even measured on site, but needs to be interpolated from other sites, or evaluated first through appropriate modeling and meteorological data. The accuracy of the predetermination of E also conditions the accuracy of E_s in this case. Since there is a large number of ways to estimate E at any site, the propagation of errors from E to E_s can be extremely difficult to evaluate. Such a specific error analysis has been left out of the scope of this study. Therefore, it is assumed here that at least E is known from on-site measurement.
If only E is known, E_{bn} and E_d must be estimated. To separate the direct and diffuse components from E, many empirical relationships have been proposed in the literature. The Orgill (21), Erbs (22), and Reindl (23) correlations are frequently used, and have therefore been selected for this study. Among the various versions of the Reindl model, the most detailed approach (where the direct/diffuse separation is made dependent on Z, ambient temperature, and relative humidity) has been selected. Note that the Erbs correlation, for instance, is part of the SSE methodology (2), and therefore partly conditions the accuracy of this dataset.

3. EXPERIMENTAL DATA

The datasets used here are from NREL's Solar Radiation Research Laboratory in Golden, Colorado (latitude 39.74°N, longitude 105.18°W, elevation 1829 m). This site is located on a mesa that overlooks the western side of the agglomeration of Denver. This is a sunny site, with an annual daily-average DNI of about 5.65 kWh/m^2. Such a resource can be classified as "relatively favorable" for solar applications. [This average DNI is close to the critical threshold of 6.0 kWh/m^2, above which the resource is generally considered favorable to the construction of solar power plants (24).]

The datasets have been obtained from SRRL's download tool, http://www.nrel.gov/midc/srrl_bms. The 1-min irradiance data used here are from the following thermopile instruments: a Kipp & Zonen (KZ) CH1 pyrheliometer to measure DNI, a KZ CM22 and an Eppley 8-48 to measure diffuse horizontal irradiance (both ventilated and with a tracking shade). The combination of the CH1 and CM22 instruments provides the "optimal" measurement dataset. An Eppley PSP with shadowband, combined with the CH1, defines a suboptimal way to obtain global irradiance. An unshaded PSP measures global horizontal radiation and

provides another source of suboptimal data. A KZ CM21 measures E_s on a 2-axis tracking plane always normal to the sun's direction, and five tilted PSPs measure E_s (i) on a south-facing tilt of 40° [nearly equal to latitude], and (ii) on vertical planes that face the four cardinal directions. Ancillary data, also measured at 1-min intervals, include: temperature, relative humidity, total cloud cover, opaque cloud cover, ground albedo, and net thermal infrared irradiance at the radiometers. The latter data is used to optimize the diffuse irradiance measurements per the correction method recently proposed (6, 25). The cloud cover information is obtained from a Yankee TSI instrument with a spatial resolution of 1% sky cover. The ground albedo is obtained as the ratio of the upwelling and downwelling global irradiance measured by two PSPs at a height of 1.6 m. The vertical, 40° and 2-axis tracking instruments are all installed on a tower, with platforms at 2.4 m, 3.4 m, and 4 m above ground, respectively. This tower is about 52 m away from the setup measuring the horizontal components.

The experimental datasets cover the 12-month period Sep 2006 to Aug 2007. Their quality has been thoroughly controlled, adding to the normal QC tests routinely performed by NREL. For instance, all data points with missing data from any sensor, with negative shortwave irradiance, with significant differences in redundant measurements, or with albedo values beyond some acceptable limits (0.05–1.0), have been rejected. A particularly insidious problem arises whenever the tilted radiometers sense direct radiation during a longer portion of the 1-min period than the horizontal ones, or vice versa. Error bounds have been used to eliminate these undesirable data points. A total of 116,942 data points met all these criteria, and served as the main database for further analysis.

The reference global horizontal irradiance, E, is calculated from E_{bn} and E_d using Eq, (2), according to the current procedure that defines optimal radiometry (6). This, and all the other steps taken to improve the measurement quality, should guarantee expanded uncertainties in E_{bn}, E_d and E better than 2.0, 5.0 and 5.4%, respectively. In addition to this "Reference" case, four alternate suboptimal input datasets have been devised:

(1) global horizontal calculated from Eq. (2) as before, but where diffuse irradiance is measured with a PSP/ shadowband combination (case noted "Shadowband");
(2) global horizontal measured with a PSP, and used with the Orgill separation method (case noted "Orgill");
(3) global horizontal measured with a PSP, and used with the Erbs separation method (case noted "Erbs");
(4) global horizontal measured with a PSP, and used with the Reindl separation method (case noted "Reindl").

These four alternate cases try to reproduce what would be typical in the practice of solar engineering calculations, i.e., use of suboptimal data.

To better evaluate how the results obtained here can be representative of other climatic conditions, the accuracy of the prediction of E_s has also been analyzed as a function of season (summer *vs* winter, conducive to high *vs* low sun), sky clarity (clear-sky *vs* all-sky conditions), snow-free ground (low albedo) *vs* snow on ground (high albedo), and ground albedo estimated at 0.2.

4. TRANSPOSITION MODELS PERFORMANCE

In this section, the *intrinsic* performance of the ten transposition models is evaluated, i.e., considering only the reference case where optimal input data are used. Each 1-min prediction of E_s via Eq. (1) is compared to its measured counterpart. This defines the individual difference between prediction and measurement, or *apparent* error of the prediction. It must be stressed that this is only an apparent error since each measured data point also carries some systematic and random error in it. The uncertainty in the tilted data is ≈3% for 2-axis global and ≈5% for the fixed tilts. The usual summary statistics (mean bias error, MBE, and root mean square error, RMSE) are obtained for each of the ten transposition models and the three tilted planes. The dataset is analyzed first as a whole, then for various possible subsets.

4.1 Overall Statistical Results

The summary statistics for all models and three tilt geometries (40°S, 90°S, and fully 2-axis tracking) appear in Table 1. These results are separated into two important groups, depending on cloud cover: (i) all-sky conditions (any cloud cover); and (ii) clear-sky conditions only (defined here as cloud amount ≤10% and DNI ≥120 W/m^2). The latter case constitutes as much as 50% of all cases, owing to the predominantly clear atmosphere.

The all-sky results in Table 1 clearly indicate that

- For the 40°S tilt, the ASHRAE and isotropic models do not perform as well as the others. [The ASHRAE model becomes isotropic whenever $s \neq 90°$.] The best results (with |MBE|<2% and RMSE≤5%) are obtained with the Gueymard and Klucher models.
- For the 2-axis tracking tilt (global normal irradiance), similar results are observed, but with slightly higher RMS values for all models except Gueymard and Perez. The former model provides the best results here.
- For the vertical tilt, the HDKR and Reindl models obtain the lowest RMS errors. The RMS error of all models is significantly more than for the 40° tilt, however. This can be related to a drastic change in the relative importance of the different components in E_s, per Eq. (1). From Eq. (2), R_r is 0.5 for a vertical tilt, but only 0.117 for s=40°. This means that the prediction of E_s for a vertical plane becomes very sensitive to any inaccuracies in the evaluation of the effective foreground albedo, or of its anisotropic features. Moreover, the mean vertical E_s is also less rich in direct radiation—about 33% less overall than what is incident on the 40° tilt, on average.

The clear-sky conditions are obviously associated with higher irradiances than those for all-sky conditions, but only 19–22% more on average because of the predominantly

clear atmosphere. The RMS errors are significantly lower under clear-sky conditions, for all models and tilts. This could be expected because clear-sky irradiances only change slowly and smoothly over one-minute intervals, and because the sky radiance is spatially much more homogeneous than under partly-cloudy conditions, for instance.

Another important aspect of these results is how they may apply to the design of solar systems. In Golden or similar sunny sites, 2-axis tracking flat-panel solar systems receive on average ≈30% more radiation than a flat-plate collector tilted at latitude. Under clear skies, this difference increases to ≈34%, and the mean annual irradiance reaches, and even exceeds, the "one sun" level commonly referred to by energy ratings, i.e., 1000 W/m^2. Under such highly favorable conditions, the Gueymard and Perez models perform consistently better than the others, for any tilt.

TABLE 1: PERFORMANCE OF ALL TRANSPOSITION MODELS WITH REFERENCE INPUT DATA

Plane	40°S		90°S		Tracking	
Model	MBE (%)	RMSE (%)	MBE (%)	RMSE (%)	MBE (%)	RMSE (%)
ALL SKY, N= 116,942						
Mean E_s (W/m^2)	643.3		432.3		836.0	
ASHRAE	-5.1	7.8	6.5	13.4	-8.1	9.6
Gueymard	-0.8	4.3	5.2	10.6	-1.0	4.2
Hay	-2.1	5.5	-2.7	8.2	-1.9	6.1
HDKR	-1.8	5.3	-0.4	7.7	-1.5	5.9
Isotropic	-5.1	7.8	-5.8	11.6	-8.1	9.6
Klucher	-1.4	4.6	0.3	8.5	-6.0	7.5
Muneer	-0.4	5.2	2.5	9.5	-5.4	7.0
Perez	-2.7	6.7	-4.7	12.0	-2.3	5.8
Reindl	-1.8	5.3	-0.4	7.7	-1.5	5.9
Skartveit	-2.4	5.7	-4.3	9.3	-2.2	6.4
CLEAR SKY, N= 58,880						
Mean E_s (W/m^2)	763.1		523.5		1019.7	
ASHRAE	-3.6	4.9	0.1	4.5	-5.5	6.2
Gueymard	-1.1	2.7	-0.2	3.8	-1.2	2.1
Hay	-1.0	3.2	-2.2	5.2	-0.3	2.7
HDKR	-0.9	3.1	-1.2	4.7	-0.1	2.7
Isotropic	-3.6	4.9	-4.9	8.1	-5.5	6.2
Klucher	-1.0	2.8	-0.5	5.1	-4.0	4.8
Muneer	0.4	2.8	2.0	5.1	-3.3	4.0
Perez	-0.7	2.6	-0.4	3.9	-1.0	2.1
Reindl	-0.9	3.1	-1.2	4.7	-0.1	2.7
Skartveit	-1.0	3.2	-2.2	5.2	-0.3	2.7

The anisotropic reflectance issues just mentioned appear even more obvious when considering the irradiance on vertical tilts of other cardinal directions, also measured at NREL. Although these cases have far less interest in solar energy applications (and are therefore not discussed in detail here), they are still important for the calculation of solar heat gains through windows. The performance of all models appears to degrade considerably when the vertical surface's azimuth changes from S to E, W and N. The concomitant spread in mean annual RMS values changes from 7.7–13.4% (Table 1) to 10.5–15.8%, 13.3–19.2%, and 14.0–36.1%, respectively. It is highly likely that a significant part of these increasingly large errors is in fact due to incorrect modeling of ground reflection, because it is normally not addressed by transposition models. The next section provides more results and discussion about the ground reflection issue.

TABLE 2: PERFORMANCE OF ALL TRANSPOSITION MODELS WITH SUBSETS OF REFERENCE DATA, SHOWING SEASON AND ALBEDO EFFECTS

Plane	40°S		90°S		Tracking	
Model	MBE (%)	RMSE (%)	MBE (%)	RMSE (%)	MBE (%)	RMSE (%)
SUMMER, no snow, N=61,669						
Mean E_s (W/m^2)	614.8		285.7		857.7	
ASHRAE	-3.2	6.1	11.2	18.9	-7.3	8.7
Gueymard	-1.1	4.1	8.4	16.1	-2.0	3.9
Hay	-2.7	4.9	-4.7	9.2	-2.7	5.0
HDKR	-2.4	4.6	-1.0	8.8	-2.4	4.8
Isotropic	-3.2	6.1	0.1	7.2	-7.3	8.7
Klucher	-0.8	4.7	7.7	11.6	-5.4	6.8
Muneer	-0.6	4.0	3.9	10.8	-5.0	6.4
Perez	-3.5	7.4	-8.7	19.4	-3.0	5.6
Reindl	-2.4	4.6	-1.0	8.8	-2.4	4.8
Skartveit	-3.0	5.0	-7.0	9.8	-2.9	5.2
WINTER, no snow, N= 36.455						
Mean E_s (W/m^2)	645.9		487.4		748.5	
ASHRAE	-8.4	10.2	6.8	12.7	-10.6	12.3
Gueymard	-1.7	4.4	4.7	8.8	-0.6	4.6
Hay	-3.5	6.2	-3.5	8.4	-3.1	7.8
HDKR	-3.2	5.9	-1.3	7.5	-2.4	7.4
Isotropic	-8.4	10.2	-10.1	13.5	-10.6	12.3
Klucher	-3.0	5.0	-3.8	7.9	-7.8	9.6
Muneer	-2.0	5.8	1.0	9.5	-7.2	9.2
Perez	-3.5	6.5	-4.1	9.9	-2.7	6.8
Reindl	-3.2	5.9	-1.3	7.5	-2.4	7.4
Skartveit	-3.8	6.5	-5.2	10.2	-3.5	8.3
WINTER, with snow, N=18,822						
Mean E_s (W/m^2)	731.6		806.1		934.1	
ASHRAE	-5.0	6.9	0.7	7.6	-6.7	8.0
Gueymard	1.6	4.4	1.9	6.3	1.6	4.2
Hay	1.9	5.5	0.5	5.9	2.2	6.3
HDKR	2.0	5.5	1.2	5.9	2.5	6.4
Isotropic	-5.0	6.9	-7.6	9.5	-6.7	8.0
Klucher	-0.6	3.7	-3.6	5.5	-5.2	6.4
Muneer	2.9	6.2	2.6	6.9	-3.9	5.4
Perez	0.7	4.8	-0.9	5.9	0.4	4.7
Reindl	2.0	5.5	1.2	5.9	2.5	6.4
Skartveit	1.7	5.6	-0.2	6.4	1.8	6.5
ALBEDO=0.2, N=116,942						
Mean E_s (W/m^2)	643.3		432.3		836.0	
ASHRAE	-5.6	8.3	3.8	18.3	-9.2	11.0
Gueymard	-1.2	4.3	2.4	15.6	-2.1	4.9
Hay	-2.5	5.3	-5.5	13.3	-3.0	6.2
HDKR	-2.2	5.1	-3.2	12.9	-2.6	6.0
Isotropic	-5.6	8.3	-8.5	19.5	-9.2	11.0
Klucher	-1.9	4.9	-2.4	16.3	-7.1	9.0
Muneer	-0.8	4.9	-0.2	13.6	-6.5	8.3
Perez	-3.2	6.7	-7.5	16.8	-3.4	6.6
Reindl	-2.2	5.1	-3.2	12.9	-2.6	6.0
Skartveit	-2.8	5.5	-7.1	14.1	-3.3	6.6

4.2 Season and Albedo Effects

The 12-month dataset has been split into two seasons, covering the periods April–August (dubbed "Summer"), and September–March (dubbed "Winter"). The "Winter" period was split into "no snow" and "snow on ground" subsets, using a threshold albedo value of 0.5. No occurrence of snow-covered ground was found in "Summer". Finally, a fourth dataset was created with all data points of any season by using a fixed albedo of 0.2 rather than the measured albedo. This is the usual simplification whenever the local albedo is not measured, i.e., in the vast majority of cases.

The interpretation of the summary statistics in Table 2 is difficult because the effect of season (and therefore solar geometry) and ground albedo is not the same for all models or tilts. Interestingly, however, all predictions for the vertical tilt appear more accurate in winter with snow-covered ground, i.e., when both the ground-reflected irradiance and E_s are at their maximum.

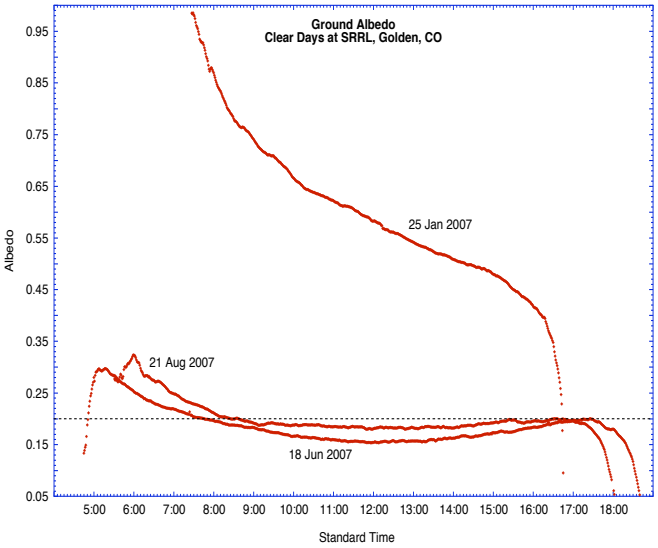

Fig. 1 Diurnal variation of ground albedo during clear days at SRRL. The dashed line indicates the constant $\rho = 0.2$.

The ground albedo varies during the day for various reasons, including departure from Lambert's Law of isotropy, and changes in ground properties (water content or snow cover). The diurnal variation of the measured albedo is shown in Fig. 1 for two clear summer days and one clear winter day. The latter case shows a rapid decrease in albedo caused by melting snow. Even the albedo of dry ground varies during the day in summer, with a minimum around noon. The morning and afternoon albedos are not symmetrical, due to inhomogeneities in ground cover. Moreover, the early morning and late evening albedos are close to zero, mostly due to artifacts, such as shading or instrumental cosine error. The winter albedo varies between 0.05 and 1.0 (because of the quality-control constraints mentioned earlier), with a mean of 0.375±0.277. Similarly, for summer, the minimum and maximum are 0.05 and 0.552, with a mean of 0.184± 0.033. The annual average albedo is 0.274, i.e., somewhat larger than the conventional value of 0.2. The immediate consequence of the uncertainty in ground reflection modeling, and of the compensation of errors that results (for some models more than others), is that it can explain (at least in part) why models perform differently from one tilt geometry to the other, or why they also perform differently from one site to the other, as the literature reveals. The present results confirm the concerns previously expressed about the importance of correctly measuring or estimating the ground-reflected irradiance (10, 12, 26, 27).

5. SUBOPTIMAL DATA UNCERTAINTY

In most practical cases of an engineering practice, the inputs to the transposition models reviewed above are not optimal, either because of the experimental inadequacies summarized in a previous study (6), or because of the uncertainties introduced by the intermediate calculations needed to obtain E_{bn} and E_d from E.

TABLE 3: ANNUAL PERFORMANCE OF SEPARATION MODELS

Component	Global		Diffuse		Direct	
Model	MBE (%)	RMSE (%)	MBE (%)	RMSE (%)	MBE (%)	RMSE (%)
ALL SKY, N=116,942						
Reference (W/m^2)	543.5		173.8		598.2	
Shadowband	-0.1	2.4	-0.2	7.5	0.0	0.0
Orgill	-0.4	4.5	-8.2	46.9	2.1	14.9
Erbs	-0.4	4.5	-10.6	47.4	2.8	15.1
Reindl	-0.4	4.5	1.1	46.6	-0.6	14.2
CLEAR SKY, N=58,880						
Reference (W/m^2)	620.5		90.6		855.1	
Shadowband	0.3	1.7	2.0	11.5	0.0	0.0
Orgill	-0.9	4.7	39.6	55.4	-4.9	7.1
Erbs	-0.9	4.7	32.3	49.5	-4.1	6.7
Reindl	-0.9	4.7	57.8	82.7	-6.8	9.1

In the Shadowband case (where global is obtained as the sum of shadowband diffuse and direct horizontal), only the diffuse measurement is suboptimal, resulting in an average RMS error of 7.5% in measured diffuse horizontal and 2.4% in derived global horizontal (Table 3). The reference DNI is used in this case, with therefore no error in what constitutes 68% of the average global horizontal irradiance.
The main input of the three direct/diffuse separation methods is the global horizontal irradiance measured here with an unventilated and thermally uncorrected pyranometer. This global radiation is less optimal than in the Shadowband case, particularly under clear skies. There are specific reasons for this, which have been discussed previously (6). As the summary statistics in Table 3 also reveal, all the separation methods introduce significant random errors in the

process, with typical RMS errors in DNI of ≈15% under all-sky conditions and 7–9% under clear-sky conditions. The performance of the Orgill and Erbs methods is similar, for both the all-sky and clear-sky cases. The Reindl method is less consistent, having the lowest RMS in the former case and the largest in the latter case. Moreover, all methods significantly underestimate DNI and overestimate diffuse under clear-sky conditions. As discussed elsewhere (28), a reason for this is the low aerosol turbidity, which is prevailing at this site but not taken into consideration by the methods. These findings confirm previous results that have been obtained for other low-turbidity locations of the Southern Hemisphere (29).

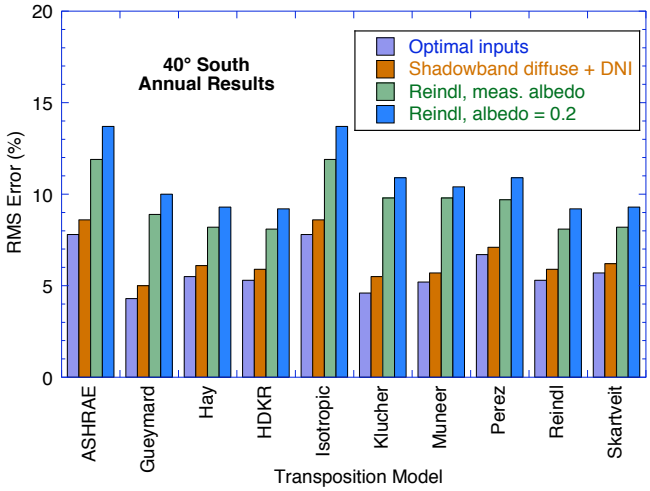

Fig. 2 Dependence of the RMS error for ten transposition models on the quality of input data for 40° tilt at SRRL.

6. SUBOPTIMAL TILTED IRRADIANCE PREDICTION

The effect on the predicted tilted radiation of combining suboptimal input data and suboptimal direct/diffuse separation is now analyzed.

As can be expected, the more the inputs deviate from optimal quality, the more the prediction error increases. This is shown in Fig. 2 for the 40°S tilt. In this case, the incident irradiance is only marginally affected by the foreground albedo, and the largest step in error increase is due to using a direct/diffuse separation model rather than measured data.

For conciseness, only a subset of annual results from all possible combinations is compiled in Table 4. The results for the Orgill correlation are nearly identical to those for the Erbs correlation and are therefore not shown.

For all cases, a comparison between Tables 1 and 4 clearly confirms the results in Fig. 2: the random error in the predicted E_s increases sharply when replacing optimal input data by suboptimal data. For all tilts, most model combinations tend to underestimate E_s. This is particularly evident in the case of the vertical plane when a fixed albedo of 0.2 is used. In that case, the RMS error also becomes large (Fig. 3). This could be expected since a vertical plane receives a relatively large fraction of ground-reflected radiation, and a fixed value of 0.2 grossly underestimates the albedo in the presence of snow. From an engineering standpoint, such an underestimation may be a good thing (to some extent), since it is on the safe or conservative side. The problem is that, *a priori*, it is difficult to know whether an underestimation or an overestimation will occur at any specific site and/or for any specific period.

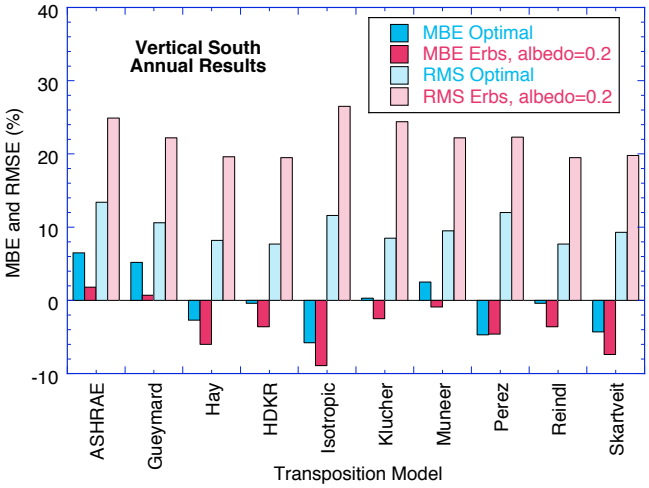

Fig. 3 Dependence of the RMS error for ten transposition models on the quality of input data for vertical tilt at SRRL.

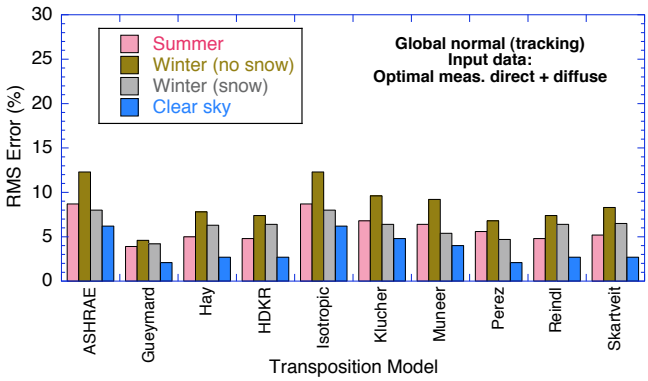

Fig. 4 Dependence of the RMS error for ten transposition models on season and sky clarity for 2-axis tracking plane.

More generally, it is nearly impossible to make recommendations about the best model combination because of the number of variables involved, the various possibilities of error cancellation, and the relative importance of bias (MBE) *vs* random errors (RMSE) in the decision process. In most cases, the intrinsic uncertainty of a transposition model becomes secondary when combined with suboptimal global radiation data, a direct/diffuse separation model, and a rough estimate of the ground albedo.

Figure 4 compares the performance results (expressed as percent RMS errors) of the ten transposition models for different seasons/conditions, the 2-axis tracking plane, and the ideal case where all inputs are optimally measured. These results can be directly compared to those of Fig. 5, rather obtained for the pragmatic case where the Erbs correlation does the direct/diffuse separation in the input data. The degradation in performance between Figs. 4 and 5 is obvious and significant. Moreover, the model performance ranking that can be attempted from the results in Fig. 4 does not translate necessarily well to the results in Fig. 5. The only possible exception is the isotropic transposition model, which consistently appears as the worst performer.

The selection of the most appropriate combination of models and albedo value ultimately conditions the performance of the whole chain of calculations. The specific performance results found here can hardly be generalized to other sites with different radiative climates. Therefore, it seems that, from a practical engineering standpoint, the current literature does not provide all the answers needed. This is because, in practice, models are not used in the ideal way they have been developed.

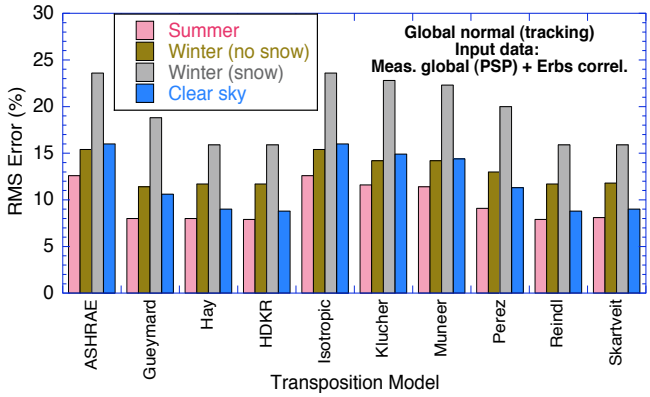

Fig. 5 Same as Fig. 4, but using suboptimal input data.

7. CONCLUSION

The results in this study show, beyond any doubt, that the major part of the uncertainty in the predicted tilted irradiance is generally caused by the direct/diffuse separation. For vertical planes and other situations where the ground-reflected radiation is a significant part of the total tilted irradiance, the accuracy of the albedo estimate becomes another key factor.

For this sunny site, and most likely for any site in a similar sunny climate, the Gueymard and Perez models provide the best estimates of global tilted irradiance when optimal input data are used. Under clear skies and ideal input conditions (measured direct + diffuse + albedo), the performance of the nine anisotropic transposition models reviewed here is within, or close to, the instrumental uncertainty limits.

TABLE 4: PERFORMANCE OF ALL TRANSPOSITION MODELS WHEN USING SUBOPTIMAL DATA

Plane	40°S		90°S		Tracking	
Model	MBE (%)	RMSE (%)	MBE (%)	RMSE (%)	MBE (%)	RMSE (%)
ALL SKY, Erbs, N= 116,942						
Mean E_s (W/m^2)	643.3		432.3		836.0	
ASHRAE	-4.8	11.9	4.3	20.1	-8.4	16.4
Gueymard	-0.8	9.3	3.2	17.5	-1.7	12.1
Hay	-2.0	8.8	-3.6	14.9	-2.3	11.3
HDKR	-1.6	8.7	-1.2	14.9	-1.9	11.2
Isotropic	-4.8	11.9	-6.5	20.3	-8.4	16.4
Klucher	-1.0	10.4	-0.1	18.8	-6.3	15.5
Muneer	-0.1	10.4	1.6	18.3	-5.8	15.3
Perez	-1.2	10.1	-2.2	17.8	-1.7	13.3
Reindl	-1.6	8.7	-1.2	14.9	-1.9	11.2
Skartveit	-2.2	8.8	-5.0	15.1	-2.6	11.3
ALL SKY, Reindl, N= 116,942						
Mean E_s (W/m^2)	643.3		432.3		836.0	
ASHRAE	-5.8	12.1	5.3	20.6	-8.7	15.5
Gueymard	-1.2	9.1	3.7	17.5	-1.5	11.3
Hay	-2.3	8.4	-3.7	14.2	-2.0	10.2
HDKR	-1.9	8.3	-1.0	14.2	-1.5	10.2
Isotropic	-5.8	12.1	-7.0	20.7	-8.7	15.5
Klucher	-1.3	10.0	0.5	18.9	-6.2	14.2
Muneer	-0.1	10.0	3.1	18.3	-5.5	13.8
Perez	-2.2	9.9	-3.5	17.4	-1.9	12.3
Reindl	-1.9	8.3	-1.0	14.2	-1.5	10.2
Skartveit	-2.5	8.4	-5.0	14.3	-2.2	10.2
ALL SKY, Erbs, Albedo=0.2, N= 116,942						
Mean E_s (W/m^2)	643.3		432.3		836.0	
ASHRAE	-5.2	12.5	1.8	24.9	-9.5	17.6
Gueymard	-1.2	9.7	0.7	22.2	-2.7	12.9
Hay	-2.3	9.1	-6.0	19.6	-3.3	11.9
HDKR	-2.0	9.0	-3.6	19.5	-2.9	11.8
Isotropic	-5.2	12.5	-8.9	26.5	-9.5	17.6
Klucher	-1.4	10.8	-2.5	24.4	-7.3	16.6
Muneer	-0.5	10.6	-0.9	22.2	-6.8	16.3
Perez	-1.6	10.5	-4.6	22.3	-2.7	14.0
Reindl	-2.0	9.0	-3.6	19.5	-2.9	11.8
Skartveit	-2.6	9.1	-7.4	19.8	-3.6	12.0
ALL SKY, Reindl, Albedo=0.2, N= 116,942						
Mean E_s (W/m^2)	643.3		432.3		836.0	
ASHRAE	-6.2	12.9	2.8	26.0	-9.7	16.9
Gueymard	-1.6	9.6	1.2	22.9	-2.5	12.3
Hay	-2.7	8.8	-6.1	19.6	-3.0	11.1
HDKR	-2.3	8.7	-3.5	19.5	-2.5	11.0
Isotropic	-6.2	12.9	-9.5	27.8	-9.7	16.9
Klucher	-1.7	10.6	-2.0	25.3	-7.2	15.6
Muneer	-0.5	10.3	0.6	22.8	-6.5	15.1
Perez	-2.6	10.4	-6.0	22.9	-2.9	13.4
Reindl	-2.3	8.7	-3.5	19.5	-2.5	11.0
Skartveit	-2.8	8.8	-7.5	19.7	-3.2	11.1

The isotropic transposition method always performs poorly, confirming most previous results of the literature. Under non-ideal conditions, the nine anisotropic transposition models perform similarly—well or poorly, depending on standpoint—overall. Their performance ranking varies as a function of receiver geometry, atmospheric conditions, season, albedo, and accuracy of the radiative inputs (measured or modeled).

It is recommended that more studies be devoted to the improvement of the complete procedure to predict tilted irradi-

ances in practice, considering the suite of necessary models as a whole, as well as the quality of their input data.

8. ACKNOWLEDGMENTS

The NREL SRRL operations and maintenance staff is thanked for their enduring hard work dedicated to providing the community with high-quality measurements. Daryl Myers kindly reviewed the manuscript and offered worthwhile comments.

9. REFERENCES

(1) Gueymard C.A. and Myers D.R., *Validation and Ranking Methodologies for Solar Radiation Models*, in *Modeling Solar Radiation at the Earth's Surface*, V. Badescu, Editor, Springer, 2008.

(2) Stackhouse P.*, et al.,* New renewable energy prototype data sets from NASA satellites and research. Proc. *Solar 2006 Conf.*, Denver, CO, American Solar Energy Society, 2006. See also http://eosweb.larc.nasa.gov/sse/.

(3) NREL, National Solar Radiation Data Base, http://rredc.nrel.gov/solar/old_data/nsrdb/.

(4) Renné D.*, et al.,* Results of solar resource assessments in the UNEP/SWERA project. Proc. *Solar World Congress*. Orlando, FL, International Solar Energy Society, 2005. See also http://swera.unep.net/.

(5) SoDa, *Services for professionals in solar energy and radiation*, http://www.soda-is.com/.

(6) Gueymard C.A. and Myers D., Performance assessment of routine solar radiation measurements for improved solar resource and radiative modeling. Proc. *Solar 2007 Conf.,* Cleveland, OH, American Solar Energy Society, 2007.

(7) Hay J.E. and McKay D.C., *Calculation of solar irradiances for inclined surfaces: verification of models which use hourly and daily data*, Report to International Energy Agency, SHCP Task IX, Atmospheric Environment Service, Canada, 1986.

(8) Kambezidis H.D.*, et al.*, Measurements and models for total solar irradiance on inclined surface in Athens, Greece. *Solar Energy*, **53**: 177-185, 1994.

(9) Psiloglou B.E.*, et al.*, Evaluation of different radiation and albedo models for the prediction of solar radiation incident on tilted surfaces, for four European locations. *Trans. ASME, J. Solar Engng.,* **118**: 183-189, 1996.

(10) Gueymard C.A., An anisotropic solar irradiance model for tilted surfaces and its comparison with selected engineering algorithms. *Solar Energy*, **38**: 367-386, 1987. Erratum, *Solar Energy*, **40**: 175, 1988.

(11) Carr A.J., *A detailed performance comparison of PV modules of different technologies and the implications for PV system design methods*, Murdoch Univ., Australia, 2005.

(12) Loutzenhiser P.G.*, et al.*, Empirical validation of models to compute solar irradiance on inclined surfaces for building energy simulation. *Solar Energy*, **81**: 254-267, 2007.

(13) ASHRAE, *Handbook of Fundamentals, SI Edition*, American Society of Heating, Refrigerating and Air-Conditioning Engineers, Atlanta, GA, 2005.

(14) Hay J.E., Calculation of monthly mean solar radiation or horizontal and inclined surfaces. *Solar Energy*, **23**: 301-307, 1979.

(15) Klucher T.M., Evaluation of models to predict insolation on tilted surfaces. *Solar Energy*, **23**: 111-114, 1979.

(16) Muneer T., ed. *Solar radiation and daylight models,* 2nd edition, Elsevier, 2004.

(17) Perez R.*, et al.*, Modeling daylight availability and irradiance components from direct and global irradiance. *Solar Energy*, **44**: 271-289, 1990.

(18) Reindl D.T.*, et al.*, Evaluation of hourly tilted surface radiation models. *Solar Energy*, **45**: 9-17, 1990.

(19) Skartveit A. and Olseth J.A., Modelling slope irradiance at high latitudes. *Solar Energy*, **36**: 333-344, 1986.

(20) Duffie J.A. and Beckman W.A., *Solar Engineering of Thermal Processes,* 2nd edition, Wiley, 1991.

(21) Orgill J.F. and Hollands K.G.T., Correlation equation for hourly diffuse radiation on a horizontal surface. *Solar Energy*, **19**: 357-359, 1977.

(22) Erbs D.G.*, et al.*, Estimation of the diffuse radiation fraction for hourly, daily and monthly-average global radiation. *Solar Energy*, **28**: 293-302, 1982.

(23) Reindl D.T.*, et al.*, Diffuse fraction correlations. *Solar Energy*, **45**: 1-7, 1990.

(24) Gueymard C.A.*, et al.*, Proposed reference irradiance spectra for solar energy systems testing. *Solar Energy*, **73**: 443-467, 2002.

(25) Michalsky J.J.*, et al.*, A proposed working standard for the measurement of diffuse horizontal shortwave irradiance. *J. Geophys. Res.,* **112D**: doi:10.1029/2007JD008651, 2007.

(26) Ineichen P.*, et al.*, Ground-reflected radiation and albedo. *Solar Energy*, **44**: 207-214, 1990.

(27) Ineichen P.*, et al.*, The importance of correct albedo determination for adequately modeling energy received by tilted surfaces. *Solar Energy*, **39**: 301-305, 1987.

(28) Gueymard C.A., Importance of atmospheric turbidity and associated uncertainties in solar radiation and luminous efficacy modelling. *Energy*, **30**: 1603-1621, 2005.

(29) Spencer J.W., A comparison of methods for estimating hourly diffuse solar radiation from global solar radiation. *Solar Energy*, **29**: 19-32, 1982.